Scientia Iranica B (2015) 22(1), 235–244

SCIENTIA IRANICA

Sharif University of Technology
Scientia Iranica
Transactions B: Mechanical Engineering
www.scientiairanica.com

Parametric study of the pressure distribution in a confined aquifer employed for seasonal thermal energy storage

H. Ghaebi, M.N. Bahadori* and M.H. Saidi

Center of Excellence in Energy Conversion (CEEC), School of Mechanical Engineering, Sharif University of Technology, Tehran, P.O. Box 11155-9567, Iran.

Received 28 November 2013; received in revised form 28 February 2014; accepted 20 April 2014

KEYWORDS
Aquifer;
Pressure distribution;
Numerical simulation;
Parametric study.

Abstract. Aquifers are underground porous formations containing water. Confined aquifers are formations surrounded by two impermeable layers. These aquifers are suitable for seasonal thermal energy storage. The objective of this research is a parametric study of the pressure distribution in an aquifer to be employed for thermal energy storage for air-conditioning of a building complex. In design of an Aquifer Thermal Energy Storage (ATES), a realistic model is needed to predict the aquifer's behavior. Here, the effects of operating parameters on pressure distribution are investigated through a three-dimensional finite difference model. In an ATES, heat transfer occurs through both convection and conduction. The convective heat transfer in ATES occurs because of pressure gradient. Therefore, knowledge of the effects of various parameters on pressure distribution is necessary. These parameters are: groundwater natural flow, the porosity and permeability of the aquifer, injection and withdrawal rates from wells, the number and the arrangements (being linear, triangular or rectangular) of injection and withdrawal wells. It has been found that variation of the pressure drop inside an aquifer with increasing permeability is very considerable in comparison with other parameters. Moreover, a validation is performed by using fluent software to verify the accuracy of the developed method.

1. Introduction

Several countries, such as the United States [1-4], Europe [5-9], and other countries [10,11], have employed confined aquifers for the seasonal storage of thermal energy for the heating and cooling of buildings. Recently, Seasonal Thermal Energy Storage (STES) systems have become more popular in the world due to the problems caused by the depletion of fossil fuels and the increase of global warming [12]. The STES systems are generally divided into a closed system (e.g., Borehole Thermal Energy Storage, BTES), and an open system (e.g., Aquifer Thermal Energy Storage, ATES). Due to its relatively high volumetric heat capacity, ATES has a higher system performance than the BTES and other systems employing low temperature geothermal heat.

Numerical modeling is a powerful tool for flow simulation in porous media such as an aquifer [13]. In the past few years, several investigations have been performed into numerical simulation of flow in aquifers. They have also applied some numerical codes, such as TRUST [14], TRUMP [15], PORFLOW [16], UNSAT [17], SUTRA [18], and MODFLOW [19], to model the aquifer system. These codes are generally based on finite difference discretization, and are used for flow and temperature distribution inside the aquifer.

Tang and Jiao [20,21] derived a two-dimensional

*. *Corresponding author. Tel./Fax: +98 21 66165583*
E-mail address: bahadori@sharif.edu (M.N. Bahadori)

analytical solution to describe the groundwater fluctuations in a leaky confined aquifer system near open tidal water. They assumed that the groundwater head in the confined aquifer fluctuates in response to the sea tide. They concluded that the groundwater response in coastal areas depends not only on the aquifer properties and structures, but also on the wave pattern. Aghbologhi et al. [22] developed a new analytical solution to describe the groundwater fluctuation in a sloping coastal aquifer system comprised of an upper unconfined aquifer, a lower confined aquifer, and an aquitard in between. The research results indicated that the effect of the bottom angle on groundwater fluctuation and time lag is significant in the unconfined aquifer and not negligible if the leakage in the confined aquifer is large. Kihm et al. [23] performed a series of three-dimensional numerical simulations using a hydro-geo-mechanical numerical model to analyze and predict fully coupled groundwater flow and land deformation due to groundwater pumping in an unsaturated fluvial aquifer system, which has irregular lateral boundaries. They used the finite element method for the analyses.

These numerical simulation results show that hydro-geo-mechanical numerical modeling can be a useful tool for analyzing and predicting long-term groundwater level fluctuations and land deformation due to groundwater pumping in actual three-dimensional aquifer systems. Shuang et al. [24] conducted a series of numerical simulations to investigate the effect of the slope of the outlet-capping on the tide-induced head fluctuations in a coastal confined aquifer. The numerical simulations demonstrated that when hydraulic diffusivity, slope and/or the outlet-capping leakages are large, tidal loading effect is relatively weak and leakage dominates. Ayvaz and Karahan [25] introduced a Simulation/Optimization (S/O) model for the identification of unknown groundwater well locations and pumping rates for two-dimensional aquifer systems. The proposed S/O model uses a finite-difference solution of the governing groundwater flow equation as its simulation model. This model is then combined with a Genetic Algorithm (GA) based optimization model which is used to determine the pumping rates for each well. The performance of the proposed S/O model is tested on two hypothetical aquifer models for both steady-state and transient flow conditions. Laplace domain solutions have been obtained for three-dimensional groundwater flow to a well in confined and unconfined wedge-shaped aquifers by Sedighi et al. [26]. The solutions take into account partial penetration effects, instantaneous drainage or delayed yield, vertical anisotropy and water table boundary condition. The results are presented in the form of dimensionless drawdown-time and boundary gradient-time type curves. Nam and Ooka [27] investigated application of a Groundwater Heat Pump (GWHP) system in an open-loop system that draws water from a well or surface water for heating/cooling of a building. In their research, 3D numerical heat transfer simulation and experiments, utilizing real-scale equipment, was conducted using a numerical code, named EFLOW, in order to develop the optimization method for GWHP systems. Simulation results were compared with the experimental ones, and the validity of the simulation model was confirmed. Dafny et al. [28] studied the influences of the geological structure (especially folding and lithology) and the karst system on the groundwater flow regime. They introduced a 3D geological-based grid for the basin for the first time. It was implemented into FEFLOW, which was used, thereafter, to analyze, quantitatively, the flow regime, the groundwater mass balance, and the aquifer hydraulic properties. Modeling results have also exhibited that in the lowland confined area, the geological structure does not play a major role in directing groundwater flow. Sensitivity analysis of a steady-state groundwater flow equation of the flow parameters and the boundary conditions, based on the perturbation approach, has been performed by Mazzilli et al. [29]. Recently, Hu et al. [30] developed a numerical model based on the Galerkin finite element method and the finite difference method for a homogeneous and isotropic confined aquifer in which a pumping well penetrates a different thickness of aquifer, and a number of full penetrating observation boreholes are placed to obtain drawdowns. They selected a hypothetical example to justify the extent and magnitude of the influences, and to demonstrate the effect of well diameter on the flow within an observation well. Their study suggests that one must be cautious in using hydraulic heads from observation wells to evaluate groundwater flow systems before the pipe-flow effect can be assumed to be negligible. Velazquez et al. [31] presented a conceptual-numerical model that can be deduced from a calibrated finite difference groundwater flow model for investigation into the response of the aquifer head distribution to surface water. Their results showed that penetration of water from the surface into the aquifer modified the pressure distribution inside the aquifer. Rushton and Brassington [32] considered the significance of the hydraulic head distribution for horizontal wells in shallow aquifers, and estimated the inflows of groundwater along the length of the well. After conceptual and computational modeling, they deduced that there are significant drawdowns in groundwater heads in the vicinity of the well. Yeh and Chang [33] summarized recent developments of flow modeling, such as the flow in aquifers, with horizontal wells or collector wells, capture zone delineation, and non-Darcian flow in porous media and fractured formations. They also presented a comprehensive review on the numerical calculations for five well functions

frequently appearing in well-hydraulic literature, and suggested some topics in groundwater flow for future research. Marion et al. [34] simulated a sharp interface model issuing from a seawater intrusion problem in a free aquifer. They also modeled the evolution of the sea front and of the upper free surface of the aquifer. They used a P1 finite element method for the space discretization combined with a semi-implicit in-time scheme.

The sub-objectives of this research paper are multiple, and include:

- Carrying out a numerical modeling for pressure distribution in an aquifer used for thermal energy storage.
- Comprehensively investigating the influence of various hydro-geological and operational parameters on pressure distribution inside an aquifer.
- Examining the use of various numbers and arrangements for injection and withdrawal wells.
- Investigating the effect of well layout on pressure distribution in the aquifer.

2. System description

In Aquifer Thermal Energy Storage (ATES), two or more wells are employed. Half of the wells are for injection and the other half for withdrawal of water. The removed water, after heat transfer with the building space, is injected back into the aquifer through the injection well(s). In winter (cold seasons), warm water and in summer (hot seasons), cold water, performs heat transfer with the building space. Figure 1 schematically shows an ATES. The aquifer considered in this study is 100 m long, 50 m wide and 6 m high, in x, y and z directions, respectively, as shown in Figure 2. It is assumed that this aquifer is homogeneous, isotropic and confined. In the base case, there is one well for injection and one well for withdrawal of water. In this case, the geological properties, dimensions of the

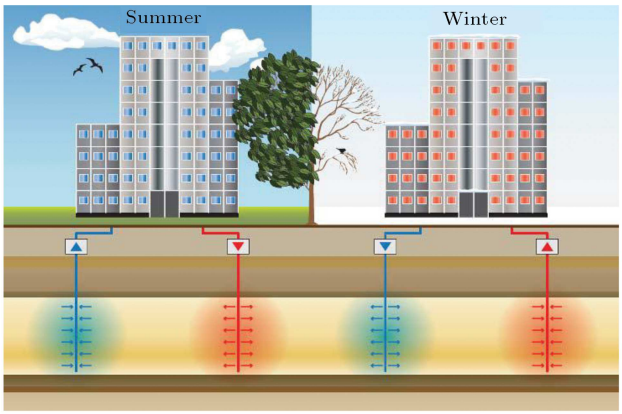

Figure 1. A schematic diagram of an ATES.

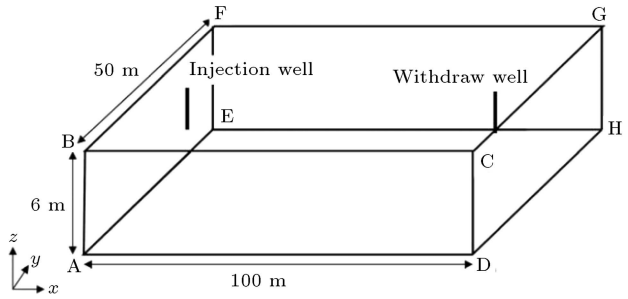

Figure 2. Three dimensional computational domain.

Table 1. Aquifer properties and well specification in the base case.

Property	Value
Permeability	$K = 0.0017\ \frac{\mathrm{m}}{\mathrm{s}}$
Porosity	0.4
Groundwater natural flow	$10\ \frac{\mathrm{m}}{\mathrm{year}}$
Water density	$1000\ \frac{\mathrm{kg}}{\mathrm{m}^3}$
Rock density	$1800\ \frac{\mathrm{kg}}{\mathrm{m}^3}$
Injection/withdraw rate	$0.74\ \frac{\mathrm{m}^3}{\mathrm{s}}$
Number of injection/withdraw well/wells	1
Location of the injection well	$x = 25$ m $y = 25$ m $z = 3$ m
Location of the withdraw well	$x = 75$ m $y = 25$ m $z = 3$ m

pumps, as well as injection and withdrawal rates, are listed in Table 1.

3. Mathematical modeling

The system considered in this study consists of a single-phase water flow inside a saturated aquifer, confined by a cap rock and a bed rock. In such a system, water flows only inside the aquifer.

An aquifer is a porous medium. Its porosity is defined as the volume of voids, or pore space, to the bulk volume of the aquifer. Porosity is expressed in terms of fraction or percentage, as:

$$\phi = \frac{V_V}{V_o}, \tag{1}$$

where ϕ, V_V and V_o are porosity, void, and the total volume of the aquifer, respectively. It is obvious that in saturated aquifers, porosity is the ratio of water volume to the total volume. The porosity of aquifers varies from 0 to 45%. For TES, 20-30% porosity is suitable [35]. By considering the porosity definition, the density of the aquifer is defined as [36]:

$$\rho = \rho_{\mathrm{Water}}\phi + \rho_{\mathrm{Rock}}(1-\phi). \tag{2}$$

Water flow is a function of the pressure distribution in the aquifer and its physical properties. In general, flow is proportional to the pressure gradient or head gradient, and the area [37]:

$$Q \propto A\frac{dh}{dL}. \tag{3}$$

This flow relationship is known as Darcy's law, and its proportionality is called permeability:

$$Q = -KA\frac{dh}{dL}. \tag{4}$$

The minus sign is necessary, because the head decreases in the direction of the flow. Another form of Darcy's law is written for the Darcy flux (or Darcy velocity, or specific velocity), which is the discharge rate per unit cross-sectional area. It is generally hard to define the velocity in an aquifer because of the existence of pores with different cross sections. The velocity in the aquifer must be a rough average number, as the cross section is never homogeneous. As a result, velocity is rarely used in geological evaluations. A velocity defined by dividing the flow rate (Q) by the aquifer cross-sectional area (A) is known as the specific velocity or V_S [37]:

$$\vec{V}_S = \frac{Q}{A} = -K\frac{dh}{dL}. \tag{5}$$

Natural flow in an aquifer is accounted for in the equations of flow. The natural flow in an aquifer can be stated as:

$$Q/A = K\vec{\Delta}h. \tag{6}$$

Practically, groundwater flows in a complex 3D pattern. Darcy's law in three dimensions is analogous to that of one dimension. In a Cartesian x, y, z coordinate system, it is commonly expressed as:

$$\vec{V}_{S,x} = -K_x\frac{\partial h}{\partial x}, \tag{7}$$

$$\vec{V}_{S,y} = -K_y\frac{\partial h}{\partial y}, \tag{8}$$

$$\vec{V}_{S,z} = -K_z\frac{\partial h}{\partial z}, \tag{9}$$

where K_x, K_y and K_z are the hydraulic conductivity in three coordinate directions of x, y and z, respectively. In general, for a given porous medium, K_x , K_y and K_z do not need to be the same in which case, the medium is called anisotropic. On the other hand, if $K_x = K_y = K_z$, the medium is called isotropic. In this study, we assume that the aquifer is isotropic.

For most natural flows, the head (h) gradient is gradual and the flow rate can be estimated readily. Natural flow rates normally vary between 1.5 to 100 $\frac{\text{m}}{\text{year}}$. To consider an aquifer for TES, the flow rates should be 10 $\frac{\text{m}}{\text{year}}$, or less [36].

The general form of the Darcy equation can be written in such a way that the effect of the gravity is taken into account [38]:

$$\vec{V}_S = -\frac{k}{\mu}\left(\vec{\Delta}h - \rho\vec{g}\right), \tag{10}$$

where $\vec{V}_S$, k and μ are specific velocity, specific permeability and viscosity, respectively, and h, ρ and $\vec{g}$ are pressure head, aquifer density and gravitational acceleration, respectively.

In ATES, charge and discharge flows are generally performed at constant rates in the operational period. Therefore, the flow is steady and the continuum equation in porous media satisfies the following equation [39]:

$$\left[\vec{\Delta}.(\rho\vec{V}_S)\right]dV = S. \tag{11}$$

S is related to the source term, and it is the rate of injection/withdrawal. In this study, it is supposed that the porosity and density are constant, hence, Eq. (11) is rewritten as:

$$\vec{\Delta}.\vec{V}_S = \frac{S(x,y,z)}{\rho dV}. \tag{12}$$

By considering Darcy's equation, $\vec{V}_S = K\nabla h$, Eq. (12) can be stated as follows:

$$\Delta^2 h = \frac{S(x,y,z)}{K\rho dV}. \tag{13}$$

4. Numerical simulation

Numerical simulations of problems in fluid dynamics are usually formulated using one of three methods: finite element, finite volume and finite difference [40]. In the finite difference approach, a finite difference approximation of the differential equation is solved. When this numerical method is applied, the equation is first transformed from the physical domain to a uniform computational domain, and the differential form of the equation is usually solved at the node points.

In this research, the finite difference approach was used for modeling the flow domain in a confined aquifer. The computational domain was three dimensional. Using the finite difference approach is conventional in ATES flow and thermal modeling. Since the boundary condition in an aquifer is simple, using the uniform structured mesh is more applicable.

The first step in a finite difference scheme is discretization. For this purpose, Eq. (13) is written as follows:

$$\frac{\partial^2 h}{\partial x^2} + \frac{\partial^2 h}{\partial y^2} + \frac{\partial^2 h}{\partial z^2} = \frac{S(x,y,z)}{K\rho dV}. \tag{14}$$

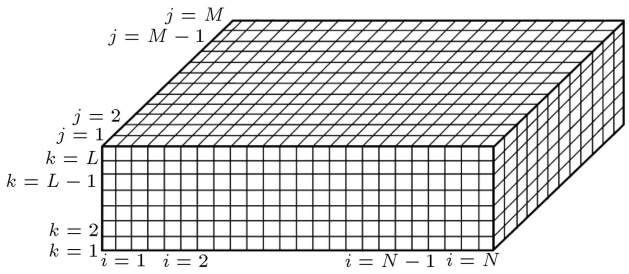

Figure 3. Meshing view.

The above equation was solved numerically using the fractional steps method in three dimensions. Initially, the equation was solved using the Crank-Nicolson implicit method, and results of the solution in one direction (for example, x direction) were used for solution in other directions (y and z directions). In any direction, the solution was performed by applying Thomas's TDMA (Three Diagonal Matrix Algorithm). A central difference scheme is used to discretize Eq. (14).

It should be noted that this method has a second order truncation error in each direction. The advantage of this procedure is its unconditional stability and higher rate of convergence, because of using the TDMA method. The more detailed discretization process is presented in Appendix A.

Meshing was performed in such a way that injection/withdrawal wells were considered in any node of the computational domain. Figure 3 shows the meshing arrangement. For investigation of mesh size independency, so that the unique solution would be obtained, several mesh sizes were examined. Finally, the mesh sizes selected were 1 m, 1 m and 0.5 m, in x, y and z directions, respectively. The dependency of the solution on mesh sizes less than these values was less than 1 percent. In this structured meshing, the number of meshes was about 67000.

To start up the solution, boundary conditions in x, y and z directions were applied. In ABFE and DCGH planes, shown in Figure 2, a pressure gradient was inserted, while the ground water flow was in the x-direction. This value of pressure gradient was obtained from Darcy's equation as follows:

$$H_{\text{imp}} = V_{gw} X_{\text{length}}/K. \tag{15}$$

The boundary conditions in ABFE and DCGH planes were as follows:

$$h_{1,j,k} = H_{\text{imp}}, \qquad h_{N,j,k} = 0. \tag{16}$$

The boundary conditions in lateral faces of ABCD and EFGH and top and bottom faces of AEHD and BFGC faces were no-penetration boundary conditions.

5. Discussion and results

Initially, the pressure distribution was calculated for the base case design. The properties of the aquifer and the locations of the injection and withdrawal wells are specified in Table 1.

In the following discussion, the pressure distribution was calculated in three dimensions. However, because of the symmetry of the domain, the pressure distribution is shown only in x direction, $y = 25$ m and $z = 3$ m. A zero pressure was arbitrarily assumed at $x = 75$ m, where water is entering the withdrawal well.

5.1. Model verification

To investigate the accuracy of the developed code, a validation was performed using FLUENT software and simulation of the computational domain. The computational domain is shown in Figure 4. In this meshing, an unstructured 3D mesh of 259346 cells was built. The chosen element was Tet/Hybrid and the type was TGrid. For verification, the head was compared with that obtained via the developed code (Table 2) between the well pairs in an x direction, at $y = 25$ m and $z = 3$ m, for the base case. The results show a good correspondence between the developed code and those obtained using FLUENT.

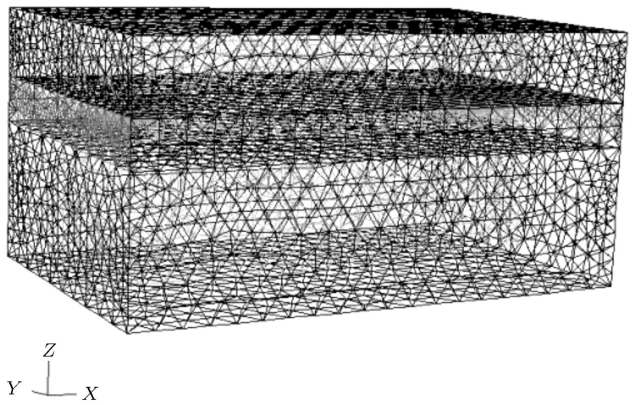

Figure 4. Model mesh in FLUENT.

Table 2. Model verification with results of FLUENT simulation.

x (m)	Head (m)		
	H_{FLUENT}	H_{Code}	Error (%)
25	14.24	13.56	4.77
30	8.26	7.72	6.53
35	7.82	7.52	3.83
40	7.55	7.14	5.43
45	7.32	6.94	5.19
50	7.08	6.83	3.53
55	6.91	6.68	3.32
60	6.69	6.47	3.28
65	6.41	6.23	2.80
70	5.98	5.86	2.01

Table 3. Effect of the variation of the groundwater velocity on the pressure distribution.

Groundwater velocity (m/year)	Maximum pressure in the aquifer (m)
10	14.1599
30	14.2065
50	14.2251
100	14.2438

5.2. The effect of groundwater natural flow on the pressure distribution between well pairs

Variation of groundwater velocity has a very low effect on the pressure distribution between well pairs. Table 3 shows the maximum pressure between well pairs (at the location of the injection well) for different groundwater velocities. Since the natural groundwater flow is considered in the x direction, the natural flow is influenced by the pressure distribution in the boundaries and in planes perpendicular to the x direction. By increasing groundwater velocity, the maximum pressure in the aquifer (at the location of the injection well) is increased (Eqs. (10), (15) and (16)) slightly, and, consequently, pressure loss between well pairs is increased as well.

5.3. The effect of porosity on the pressure distribution between well pairs

Figure 5 shows the pressure distribution between well pairs, with respect to porosity. As seen, by increasing the porosity, the pressure losses are increased. This happens because the increment in porosity tends to increase the void space inside the aquifer and the higher flow rate between wells.

5.4. The effect of permeability on the pressure distribution between well pairs

Hydraulic conductivity (permeability) is the ability of porous media to transmit water. It should be noted that the hydraulic conductivity implies hydraulic resistance of an aquifer. Figure 6 shows the variation of pressure distribution, with respect to permeability. As permeability increases, the hydraulic resistance with respect to flow is decreased. As a result, the pressure loss between wells is decreased. According to Eq. (10), lower flow occurs because of lower pressure differences.

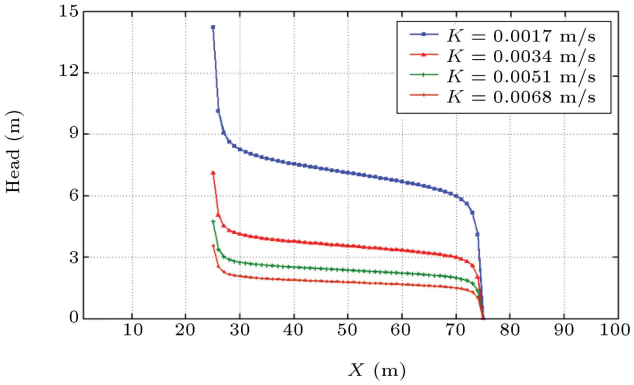

Figure 6. Variation of pressure distribution between well pairs with permeability at $y = 25$ and $z = 3$ m, and for $\phi = 0.4$, $V_{gw} = 10\frac{\text{m}}{\text{year}}$ and $Q = 0.74\frac{\text{m}^3}{s}$.

5.5. The effect of injection/withdrawal rate on the pressure distribution between well pairs

Figure 7 shows the effects of injection/withdrawal rates on the pressure distribution. The injection/withdrawal rate is the source term in the pressure distribution equation. As shown in Eq. (14), by increasing flow rate, pressure losses are increased. It should be noted that in this research, the injection rate is the same as the withdrawal rate.

5.6. The effect of number and arrangement of wells on the pressure distribution between well pairs

In the previous sections, one pair of injection/withdrawal wells was used. An objective of this research was

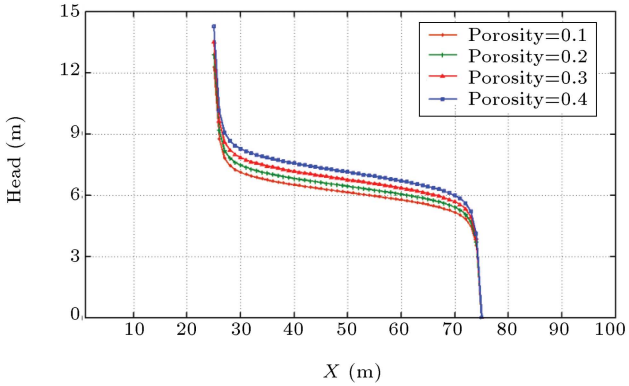

Figure 5. Variation of pressure distribution between well pairs with porosity at $y = 25$ and $z = 3$ m, and for $K = 0.0017\frac{\text{m}}{\text{s}}$, $V_{gw} = 10\frac{\text{m}}{\text{year}}$ and $Q = 0.74\frac{\text{m}^3}{s}$.

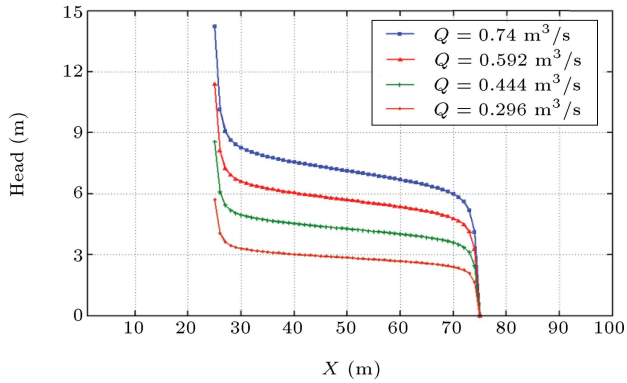

Figure 7. Variation of pressure distribution between well pairs with injection/withdrawal flow rate at $y = 25$ and $z = 3$ m, and for $K = 0.0017\frac{\text{m}}{\text{s}}$, $V_{gw} = 10\frac{\text{m}}{\text{year}}$ and $\phi = 0.4$.

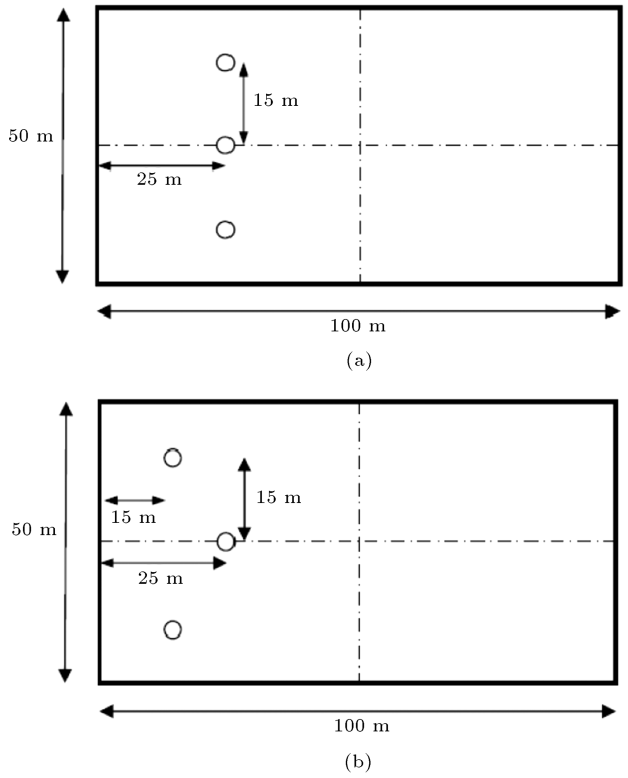

Figure 8. A three-well application: a) Linear arrangement; and b) triangular arrangement.

to investigate the effects of number and the arrangement of wells (being linear, triangular and rectangular) on pressure distribution inside the aquifer.

5.6.1. A three-well arrangement

Figure 8 shows the dimensions and the arrangements of three wells employed for injection, and three wells used for the withdrawal of water. The arrangements can be linear or triangular, as shown in Figure 8(a) and (b), respectively.

Pressure distribution in the aquifer is shown in Figure 9 in a three-well application. As seen, pressure losses in the linear array are more than in the triangular arrangement.

5.6.2. A five-well arrangement

Figure 10 shows the arrangement of a five-well application. In this case, the array can be linear, triangular or rectangular, as shown in Figure 10(a), (b) and (c), respectively.

Figure 11 shows the pressure distribution in a five-well application. As seen, pressure losses in the linear arrangement are slightly higher.

6. Conclusion

A parametric study of pressure distribution in a confined aquifer employed for seasonal thermal energy storage was carried out in this research. The effects of

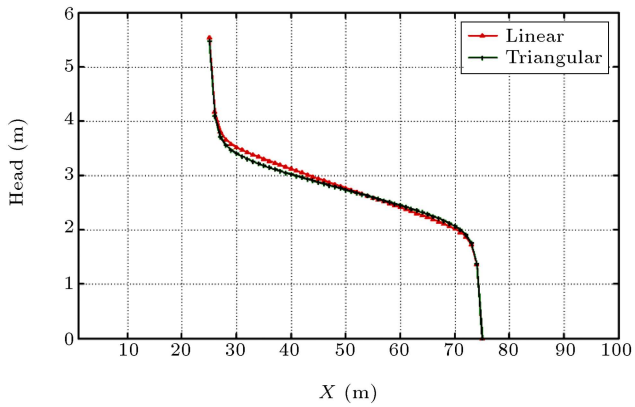

Figure 9. Pressure distribution between well pairs in a three-well application for $K = 0.0017\frac{\text{m}}{\text{s}}$, $V_{gw} = 10\frac{\text{m}}{\text{year}}$, $\phi = 0.4$ and $Q = 0.74\frac{\text{m}^3}{s}$.

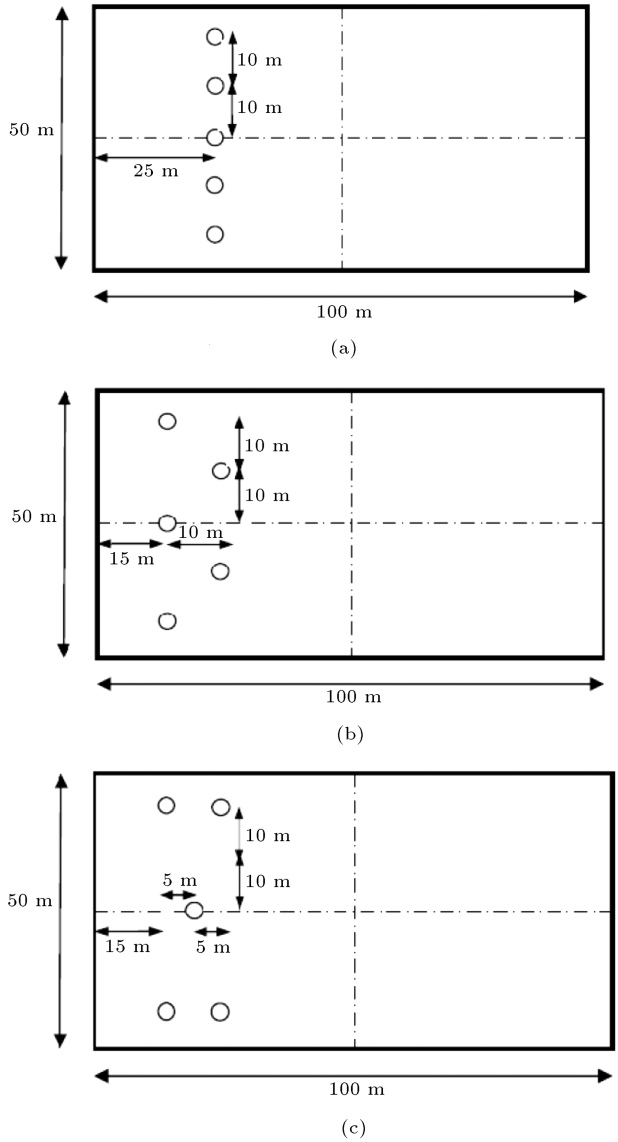

Figure 10. A five-well application: a) Linear arrangement; b) triangular arrangement; and c) rectangular arrangement.

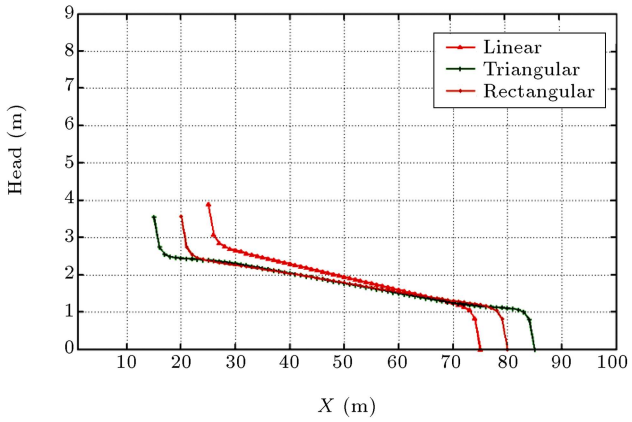

Figure 11. Pressure distribution between well pairs in a five-well application for $K = 0.0017\frac{\mathrm{m}}{\mathrm{s}}$, $V_{gw} = 10\frac{\mathrm{m}}{\mathrm{year}}$, $\phi = 0.4$, $Q = 0.74\frac{\mathrm{m}^3}{s}$.

the groundwater natural flow, porosity, permeability, injection and withdraw rates, numbers and arrangements (linear, triangular and rectangular) of wells were investigated. The following conclusions may be drawn from this research:

- By increasing the natural flow of ground water, pressure loss in the aquifer increases.
- An increase of porosity leads to lowering of the pressure loss.
- As permeability increases, the pressure loss in the aquifer decreases.
- As injection/withdraw rates increase, the pressure loss increases.
- When the number of wells increases, while the total injection/withdraw rates remain unchanged, the pressure loss increases.
- The pressure losses in the linear three-well and five-well arrangements are higher than when the arrangements are triangular and rectangular.

References

1. Meyer, C.F. and Todd, D.K. "Heat storage wells", *Water Well Journal*, **10**, pp. 35-41 (1973).
2. Molz, F.J., Warman, J.C. and Jones, T.E. "Aquifer storage of heated water: Part 1: A field experiment", *Ground Water*, **16**, pp. 234-241 (1978).
3. Papadopulos, S.S. and Larson, S.P. "Aquifer storage of heated water: Part 2: Numerical simulation of field results", *Ground Water*, **16**, pp. 242-248 (1978).
4. Parr, D.A., Molz, F.J. and Melville, J.G. "Field determination of aquifer thermal energy storage parameters", *Ground Water*, **21**, pp. 22-35 (1983).
5. Sanner, B., Karytsas, C., Mendrinos, D. and Rybach, L. "Current status of ground source heat pumps and underground thermal energy storage in Europe", *Geothermics*, **32**, pp. 579-588 (2003)
6. Paksoy, H.O., Andersson, O., Abaci, S., Evliya, H. and Turgut, B. "Heating and cooling of a hospital using solar energy coupled with seasonal thermal energy storage in an aquifer", *Renewable Energy*, **19**, pp. 117-122 (2000).
7. Dickinson, J.S., Buik, N., Matthews, M.C. and Snijders, A. "Aquifer thermal energy: Theoretical and operational analysis", *Geotechnique*, **59**, pp. 249-260 (2009).
8. Novo, V.A., Bayon, R.J., Castro-Fresno, D. and Rodriguez-Hernandez, R. "Review of seasonal heat storage in large basins: Water tanks and gravel water pits", *Applied Energy*, **87**, pp. 390-397 (2010).
9. Preene, M. and Powrie, W. "Ground energy systems: Delivering the potential", *Energy*, **34**, pp. 77-84 (2009).
10. Umemiya, H. and Satoh, Y. "A cogeneration system for a heavy-snow fall zone based on aquifer thermal energy storage", *Japanese Society of Mechanical Engineering*, **33**, pp. 757-765 (1990).
11. Lee, K.S. "Performance of open borehole thermal energy storage system under cyclic flow regime", *Journal of Geoscience*, **12**, pp. 169-175 (2008).
12. Rosen, M.A. "Second-law analysis of aquifer thermal energy storage systems", *Energy*, **24**, pp. 167-182 (1999).
13. Shamsai, A. and Vosoughifar, H.R. "Finite volume discretization of flow in porous media by MATLAB system", *Scientia Iranica*, **11**, pp. 146-153 (2004).
14. Narasimhan, T.N. "TRUST: A computer program for transient and steady state fluid flow in multidimensional variably saturated deformable media under isotherm conditions", *Lawrence Berkeley Laboratory Memorandum* (1984).
15. Schauer, D.A. "FED: A computer program to generate geometric input for the heat transfer code TRUMP", Report UCRL-50816 (1973).
16. Runchal, A.K. "PORFLOW: A software tool for multi phase fluid flow, heat and mass transport in fractured porous media, user's manual version 2.50", *Analytical & Computational Research*, Inc., Los Angeles, CA 90077 (1984).
17. Fayer, M. and Jones, T. "UNSAT-H version 2.0: Unsaturated soil water and heat flow model", PNL-6779, Pacific Northwest Laboratory, Richland, Washington (1990).
18. Souza, W.R. "Documentation of a graphical display program for the saturated-unsaturated transport (SUTRA) finite element simulation model", U.S. Geological Survey Water-Resource Investigation Report 874245 (1987).
19. Jobson, H.E. and Harbaugh, A.W. "Modifications to the diffusion analogy surface-water flow model (daflow)

for coupling to the modular finite-difference groundwater flow model (Modflow)", U.S. Geological Survey Open-File Report 99-217 (1999).

20. Tang, Z. and Jiao, J.J. "A two-dimensional analytical solution for groundwater flow in a leaky confined aquifer system near open tidal water", *Hydrological Processes*, **15**, pp. 573-585 (2001).

21. Jiao, J.J. and Tang, Z. "An analytical solution of groundwater response to tidal fluctuation in a leaky confined aquifer", *Water Resources Research*, **35**, pp. 747-751 (1999).

22. Aghbolaghi, M.A., Chuang, M.H. and Yeh, H.D. "Groundwater response to tidal fluctuation in a sloping leaky aquifer system", *Applied Mathematical Modelling*, **36**, pp. 4750-4759 (2012).

23. Kihm, J.H., Kim, J.M., Sung-Ho, S. and Gyu-Sang, L. "Three-dimensional numerical simulation of fully coupled groundwater flow and land deformation due to groundwater pumping in an unsaturated fluvial aquifer system", *Journal of Hydrology*, **35**, pp. 1-14 (2007).

24. Shuang, L., Hailong, L., Boufadel, M.C. and Guohui, L. "Numerical simulation of the effect of the sloping submarine outlet-capping on tidal groundwater head fluctuation in confined coastal aquifers", *Journal of Hydrology*, **36**, pp. 339-348 (2008).

25. Ayvaz, M.T. and Karahan, H. "A simulation/ optimization model for the identification of unknown groundwater well locations and pumping rates", *Journal of Hydrology*, **35**, pp.76-92 (2008).

26. Sedghi, M.M., Samani, N. and Sleep, B. "Three-dimensional semi-analytical solution to groundwater flow in confined and unconfined wedge-shaped aquifers", *Advances in Water Resources*, **32**, pp. 925-935 (2009).

27. Nam, Y. and Ooka, R. "Numerical simulation of ground heat and water transfer for groundwater heat pump system based on real-scale experiment", *Energy and Buildings*, **42**, pp. 69-75 (2010).

28. Dafny, E., Burg, A. and Gvirtzman, H. "Effects of karst and geological structure on groundwater flow: The case of Yarqon-Taninim aquifer, Israel", *Journal of Hydrology*, **38**, pp. 260-275 (2010).

29. Mazzilli, N., Guinot, V. and Jourde, H. "Sensitivity analysis of two-dimensional steady-state aquifer flow equations. Implications for groundwater flow model calibration and validation", *Advances in Water Resources*, **33**, pp. 905-922 (2010).

30. Hu, L., Chen, C. and Chen, X. "Simulation of groundwater flow within observation boreholes for confined aquifers", *Journal of Hydrology*, **39**, pp. 101-108 (2011).

31. Velazquez, D.P., Sahuquillo, A. and Andreu, J. "A conceptual-numerical model to simulate hydraulic head in aquifers that are hydraulically connected to surface water bodies", *Hydrological Process*, **25**, DOI: 10.1002/hyp.8214 (2011).

32. Rushton, K.R. and Brassington, F.C. "Significance of hydraulic head gradients within horizontal wells in unconfined aquifers of limited saturated thickness", *Journal of Hydrology*, **49**, pp. 281-289 (2013).

33. Yeh, H.D. and Chang, Y.Ch. "Recent advances in modeling of well hydraulics", *Advances in Water Resources*, **51**, pp. 27-51 (2013).

34. Marion, P., Najib, K. and Rosier, C. "Numerical simulations for a seawater intrusion problem in a free aquifer", *Applied Numerical Mathematics*, **75**, pp. 48-60 (2014).

35. Tsang, C.F., *Aquifer Thermal Energy Storage, A Survey*, LBL Report, USA (1980).

36. Schaetzle, W.J., *Thermal Energy Storage in Aquifers, Design and Applications*, Pergamon Press, UK (1980).

37. Strack, O.D.L., *Groundwater Mechanins*, Prentice Hall, USA (1989).

38. Kangas, M.T. and Lund, P.D. "Comparison of long term ATES experiment to 3-D computer simulation", *Proceeding of 26th International Energy Conversion Conference*, Boston, MA, USA (1985).

39. Kangas, M.T. and Lund, P.D. "Modeling and simulation of aquifer storage energy system", *Solar Energy*, **53**, pp. 237-247 (1994).

40. Bear, J., *Dynamic of Fluids in Porous Media*, Elsevier, Dover Publication. Inc. publisher, pp. 450-510 (1992).

41. Hoffmann, K.A. and Chiang, S.T., *Computational Fluid Dynamic*, Publication of Engineering education System, USA (2000).

Appendix A

By defining the following parameters:

$$E_x = \frac{1}{\Delta x^2}, \tag{A.1}$$

$$E_y = \frac{1}{\Delta y^2}, \tag{A.2}$$

$$E_z = \frac{1}{\Delta z^2}. \tag{A.3}$$

Eq. (14) is discretized, as follows, in the functional steps method [41]:

Sweeping in x direction:

$$\left(\frac{E_x}{2}\right) h^*_{i+1,j,k} - (E_x)\, h^*_{i,j,k} + \left(\frac{E_x}{2}\right) h^*_{i-1,j,k} = \frac{S_{i,j,k}}{K\rho dV} - \left(\frac{E_x}{2}\right) h^n_{i+1,j,k} + (E_x + E_y + E_z)\, h^n_{i,j,k}$$

$$-\left(\frac{E_x}{2}\right)h^n_{i-1,j,k}-(E_y)\,h^n_{i,j+1,k}-(E_y)\,h^n_{i,j-1,k}$$
$$-(E_z)\,h^n_{i,j,k+1}-(E_z)\,h^n_{i,j,k-1}. \quad (A.4)$$

Sweeping in y direction:

$$\left(\frac{E_y}{2}\right)h^{**}_{i,j+1,k}-(E_y)\,h^{**}_{i,j,k}+\left(\frac{E_y}{2}\right)h^{**}_{i,j-1,k}$$
$$=\frac{S_{i,j,k}}{K\rho_a dV}-\left(\frac{E_x}{2}\right)h^*_{i+1,j,k}+(E_x)\,h^*_{i,j,k}$$
$$-\left(\frac{E_x}{2}\right)h^*_{i-1,j,k}-\left(\frac{E_x}{2}\right)h^n_{i+1,j,k}$$
$$+(E_x+E_y+E_z)\,h^n_{i,j,k}-\left(\frac{E_x}{2}\right)h^n_{i-1,j,k}$$
$$-\left(\frac{E_y}{2}\right)h^n_{i,j+1,k}-\left(\frac{E_y}{2}\right)h^n_{i,j-1,k}$$
$$-(E_z)\,h^n_{i,j,k+1}-(E_z)\,h^n_{i,j,k-1}. \quad (A.5)$$

Sweeping in z direction:

$$\left(\frac{E_z}{2}\right)h^{n+1}_{i,j,k+1}-(E_z)\,h^{n+1}_{i,j,k}+\left(\frac{E_z}{2}\right)h^{n+1}_{i,j,k-1}$$
$$=\frac{S_{i,j,k}}{K\rho dV}-\left(\frac{E_x}{2}\right)h^*_{i+1,j,k}+(E_x)\,h^*_{i,j,k}$$
$$-\left(\frac{E_x}{2}\right)h^*_{i-1,j,k}-\left(\frac{E_x}{2}\right)h^n_{i+1,j,k}$$
$$+(E_x+E_y+E_z)\,h^n_{i,j,k}-\left(\frac{E_x}{2}\right)h^n_{i-1,j,k}$$
$$-\left(\frac{E_y}{2}\right)h^{**}_{i,j+1,k}+(E_y)\,h^{**}_{i,j,k}$$
$$-\left(\frac{E_y}{2}\right)h^{**}_{i,j-1,k}-\left(\frac{E_y}{2}\right)h^n_{i,j+1,k}$$
$$-\left(\frac{E_y}{2}\right)h^n_{i,j-1,k}-\left(\frac{E_z}{2}\right)h^n_{i,j,k+1}$$
$$-\left(\frac{E_z}{2}\right)h^n_{i,j,k-1}. \quad (A.6)$$

It should be noted that n and $n+1$ are related to two successive iterations.

Biographies

Hadi Ghaebi is currently a PhD degree student at Sharif University of Technology, Tehran, Iran. His research areas include thermal system design and optimization, renewable energy technologies, net zero energy buildings and hydrogen and fuel cells.

Mehdi Bahadorinejad received his PhD degree in Mechanical Engineering from the University of Illinois, USA, in 1964, and is currently Professor of Mechanical Engineering at Sharif University of Technology, Tehran, Iran. His research interests include natural cooling systems, solar energy utilization, environmentally- compatible energy systems, development of indigenous technology, application of scientific-spiritual thinking to social problems, entropy and awareness and engineering ethics and engineering of ethics.

Mohammad Hassan Saidi is Professor in the School of Mechanical Engineering at Sharif University of Technology, Tehran, Iran. His current research interests include MEMS, heat transfer enhancement in boiling and condensation, modeling of pulse tube refrigeration, vortex tube refrigerators, indoor air quality and clean room technology, energy efficiency in home appliances, and desiccant cooling systems.